ELSEVIER

Epilepsy Research 61 (2004) 73–87

Epilepsy Research

www.elsevier.com/locate/epilepsyres

Impulse response function based on multivariate AR model can differentiate focal hemisphere in temporal lobe epilepsy

Fumikazu Miwakeichi[a,*], Andreas Galka[b,c], Sunao Uchida[d], Hiroshi Arakaki[e], Nobuhide Hirai[f], Masaki Nishida[f], Taketoshi Maehara[g], Kensuke Kawai[h], Shigeki Sunaga[h], Hiroyuki Shimizu[h]

[a] *Laboratory for Dynamics of Emergent Intelligence, RIKEN Brain Science Institute, Saitama, Japan*
[b] *Department of Prediction and Control, The Institute of Statistical Mathematics, Tokyo, Japan*
[c] *Institute of Experimental and Applied Physics, Christian-Albrechts-University of Kiel, Germany*
[d] *Department of Sport Science, School of Sport Sciences, Waseda University, Saitama, Japan*
[e] *Department of Psychiatry and Behavioral Science, Tokyo Medical and Dental University, Tokyo, Japan*
[f] *Department of Psychiatry, Jichi Medical School, Tochigi, Japan*
[g] *Department of Neurosurgery, Tokyo Medical and Dental University, Tokyo, Japan*
[h] *Department of Neurosurgery, Tokyo Metropolitan Neurological Hospital, Tokyo, Japan*

Received 28 February 2004; received in revised form 4 June 2004; accepted 13 June 2004
Available online 17 August 2004

Abstract

The purpose of this study is to propose and investigate a new approach for discriminating between focal and non-focal hemispheres in intractable temporal lobe epilepsy, based on applying multivariate time series analysis to the discharge-free background brain activity observed in nocturnal electrocorticogram (ECoG) time series.

Five unilateral focal patients and one bilateral focal patient were studied. In order to detect the location of epileptic foci, linear multivariate autoregressive (MAR) models were fitted to the ECoG data; as a new approach for the purpose of summarizing these models in a single relevant parameter, the behavior of the corresponding impulse response functions was studied and described by an attenuation coefficient.

In the majority of unilateral focal patients, the averaged attenuation coefficient was found to be almost always significantly larger in the focal hemisphere, as compared to the non-focal hemisphere. Also the amplitude of the fluctuations of the attenuation coefficient was significantly larger in the focal hemisphere. Moreover, in one patient showing a typical regular sleep cycle, the attenuation coefficient in the focal hemisphere tended to be larger during REM sleep and smaller during Non-REM sleep. In the bilateral focal patient, no statistically significant distinction between the hemispheres was found.

* Corresponding author. Tel.: +81 48 462 1111x7425;
fax: +81 48 467 6938.
E-mail address: miwake1@brain.riken.go.jp (F. Miwakeichi).

doi:10.1016/j.eplepsyres.2004.06.003

This study provides encouraging results for new investigations of brain dynamics by multivariate parametric modeling. It opens up the possibility of relating diseases like epilepsy to the properties of inconspicuous background brain dynamics, without the need to record and analyze epileptic seizures or other evidently pathological waveforms.

Keywords: Temporal lobe epilepsy; Electrocorticogram (ECoG); Basic background activity; Multivariate autoregressive (AR) model; Impulse response function; Attenuation coefficient; Detection of epileptic hemisphere

1. Introduction

The electroencephalogram (EEG) is the reflection upon the scalp of the summed synaptic potentials of millions of neurons (Lopes da Silva, 1987; Speckmann and Elger, 1987). Depending on the presence of different cognition processes or diseases in brain, various kinds of typical waveforms and patterns appear in the EEG. In the field of epileptology, the EEG has been found to be a useful tool for detecting those regions that contain epileptic foci. In cases where unambiguous localization is difficult, the EEG recorded at intracranial electrodes is frequently investigated (Niedermeyer, 1987).

Recently, surgical treatment of temporal lobe epilepsy has found widespread application. For the evaluation of surgical indication for the treatment of epilepsy, both imaging techniques (MRI and/or SPECT) and EEG recordings (including foramen ovale) are employed.

It is well known in physiology that there exists a pronounced relationship between epileptic discharges and sleep stages (Velasco et al., 1995). In most epileptic patients, Non-REM sleep promotes the occurrence of inter-ictal epileptiform electric discharges (spikes). Therefore, in many cases, the epileptic focal hemisphere can be detected by investigating spike rates and phase delays between channels in Non-REM sleep. On the other hand, there is only little spiking activity during REM periods (Montplaisir et al., 1987; Wieser, 1991; Chokroveerty, 1994).

For the majority of patients, the laterality of the epileptic focus or foci can be consistently determined by using these sources of information. However, it is also known that not always a higher spike rate will reliably indicate the epileptic hemisphere, and in difficult cases the analysis may yield ambiguous or contradictory results, such that further evaluation is required prior to surgery. In such cases, the electrocorticogram (ECoG), recorded at subdural electrodes, can provide essential information for the localization of epileptic foci (Shimizu et al., 1992). However, since these electrodes are usually implanted for less than 2 weeks, it is not always possible to record a typical epileptic seizure during this period of time. Analysis of inter-ictal spike discharges may provide additional information, but not always can the focal hemisphere be correctly identified from higher density of inter-ictal spike discharges. Thus, it would be desirable to develop new approaches for the analysis of EEG and ECoG time series that are capable of extracting relevant information from background brain activity without any necessity for analyzing seizures or spikes.

Already by visual inspection of inter-ictal ECoG, it is possible to observe differences of the basic background activity between hemispheres. So far there have been only few studies that characterize the dynamics of the background activity of EEG or ECoG time series in epileptic patients. Within the framework of parametric modeling, such analysis requires the explicit or implicit choice of a model class for the dynamics. One has to choose between the two cases of linear or nonlinear dynamics, and also between the two cases of deterministic or stochastic dynamics, such that altogether four basic classes can be distinguished. Among these classes, the linear deterministic case can easily be discarded, since it describes only a small number of very simple waveforms (Hamilton, 1994).

In the last two decades, the class of nonlinear deterministic dynamics (including “chaotic” dynamics) has been employed frequently for the analysis of EEG or ECoG time series. A famous analysis approach, implicitly anticipating this model class, is the estimation of the correlation dimension D2 (Grassberger and Procaccia, 1983), which is interpreted as a measure of neural complexity. A characteristic decrease of D2 (i.e. a neural complexity loss) in the focal hemisphere of epileptic patients has been reported (Lehnertz and Elger, 1995; Weber et al., 1998).

The main disadvantage of D2 as a measure for describing EEG/ECoG dynamics lies in the fact that the assumption of determinism has to be regarded as inappropriate for brain dynamics. Furthermore, this measure has been found to be very susceptible to a variety of imperfections in the data, such as noise and nonstationarities; a detailed study of these problems can be found in Galka (2000).

Nonlinear stochastic models form the most general model class, but this model class cannot be employed directly without additional explicit assumptions. The linear approximation to this general class (i.e. the linear stochastic case) is widely known as a well-defined and useful first-order approximation for general nonlinear dynamics, deferring explicitly nonlinear terms to higher orders of approximation. This model class, represented by the well-known class of (linear) autoregressive (AR) models, has been applied to EEG time series by various authors already in the 1970s (for a review of the early work, see Isaksson et al., 1981). Soon linear stochastic modeling was extended to the case of multivariate time series, such that all available electrodes of EEG or ECoG recordings could be employed simultaneously (Gersch et al., 1977; Akaike, 1981); the corresponding generalization of AR models is known as multivariate AR (MAR) models. Several studies have employed MAR modeling of EEG/ECoG time series for purposes of spectral estimation, coherence analysis and information flow quantification (Kaminski and Blinowska, 1991; Gath et al., 1992; Franaszczuk and Bergey, 1998; Medvedev and Willoughby, 1999). There are also applications of MAR modeling to the prediction of the effects of surgery on the EEG (Akiyama et al., 1995) and to hierarchical decomposition of EEG/ECoG time series into source processes (Repucci et al., 2001). With respect to data recorded from epileptic patients, most of these studies focused exclusively on analyzing the ictal EEG. Hernandez et al. (1996) and Miwakeichi et al. (2001) presented successful approaches to modeling epileptiform wave shapes by non-parametric models, and in this context, Miwakeichi et al. (2001) introduced as a generalization structured non-parametric modeling.

In the present study, we discuss the concept of modeling ECoG data recorded during sleep by linear MAR models, in order to characterize dynamical properties of focal and non-focal hemispheres in epileptic patients. Certain phenomena in ECoG data, such as spike-wave patterns, cannot be described well within this model class, since for this task nonlinear elements would be required (Miwakeichi, 2001); but this does not represent a serious limitation of our approach, since in this paper our interest lies exclusively in the background dynamics and not in epileptiform wave shapes.

We remark that the estimation of MAR models is much less demanding in terms of computational time and memory consumption than typical nonlinear methods, such as the estimation of D2; therefore, it can be easily applied also to very long datasets, such as nocturnal ECoG data.

It is a characteristic problem of MAR models that they may contain a comparatively large number of model parameters, which cannot directly be employed for the purpose of characterizing the dynamics. Therefore, methods for further summarizing and condensing the information contained in MAR models are required. One approach consists of transforming the model to frequency domain; then, causality and coherence can be quantified through the noise contribution algorithm or cross-spectral methods (Gersch et al., 1977; Akaike, 1981; Liberati et al., 1997). However, when employing these techniques, still the number of resulting spectral parameters for each frequency will be of the order of the number of EEG channels squared.

When attempting to investigate time-varying dynamics from nocturnal ECoG by these models, this problem becomes even more severe. Therefore, we propose to characterize the MAR model by using its impulse response function. In the present study, we will feasibly summarize MAR models by a single parameter, called attenuation coefficient, which will be based on averaging the impulse response function over channels.

In this paper, we will develop the modeling and analysis approach and present results of a preliminary study based on sleep ECoG data from six patients suffering from temporal lobe epilepsy. While the numbers of available patients and of subdural electrodes do not yet suffice for a full-scale study of clinical usefulness, nevertheless the comparison of our results with a more traditional measure, the spike rate, and with the corresponding hypnograms reveals interesting tendencies and encourages further work along these lines.

2. Methods

2.1. Patient selection

Intracranial recordings of six patients with medically intractable temporal lobe epilepsy were studied (two male and four female; age 25–45 years). All patients were candidates for neurosurgical treatment and gave informed consent for nocturnal ECoG recording.

In all of these patients, the results of identifying the focal hemisphere by imaging techniques (MRI and/or SPECT) and EEG recordings (including foramen ovale electrodes) were either contradictory or ambiguous, therefore invasive ECoG recordings were employed.

Localization of the epileptic foci was carried out by considering the overall results of clinical examinations. The results are summarized in Table 1. For conclusively discriminating focal and non-focal hemispheres, the results of surgical treatment are most relevant. Video-ECoG recordings were done in all cases; all seizure ECoG recordings corresponded to clinical seizures according to the simultaneous video recordings. Inter-ictal spike frequency was counted by visual inspection of printouts of the clinical recordings.

Histopathological examination showed abnormal results for all unilateral patients, in particular hippocampal sclerosis (#1, #2, #3) and hippocampal gliosis (#5, #6) were found. After temporal lobectomy four of the five unilateral patients became seizure-free. The remaining unilateral patient (#3) continues to have generalized tonic–clonic seizures after surgery, although the rate of seizures has been substantially reduced from one to three times per month to one to two times per year. Patient #5 had two foci in right mesiobasal and left inferior temporal gyrus (T3) areas. In this case, the ECoG results indicated that all recorded seizures originated from the right mesiobasal focus. For patient #4, according to the EEG the spike rate in the left hemisphere was higher than in the right, however, no clear abnormalities were found in MRI and SPECT. From video-ECoG, it was gleaned that ictal discharges were initialized ten times in the left mesial temporal lobe and nine times in the right. Therefore, the case of patient #4 was diagnosed as bilateral mesiotemporal epilepsy. In summary, five unilateral focal patients (two left-sided, three right-sided) and one bilateral focal patient were studied.

2.2. Data acquisition and spike detection

Subdural electrodes were attached to cortical areas and the parahippocampal gyrus for the clinical purpose of evaluating the foci of epileptic seizures. Specially designed T-shaped sets of eight electrodes were attached in order to record parahippocampal and basal temporal cortical activities from both hemispheres (Shimizu et al., 1992) (Fig. 1). In this study, ECoG recorded from these T-shaped sets of electrodes was analyzed. The method of recording was bipolar; as shown in panel B of Fig. 1, the number of channels was six on each temporal lobe.

Polysomnographic recordings were also made in order to evaluate sleep stages. In addition to ECoG also EEG (at position Cz), oblique electrooculogram and chin electromyogram were recorded. Sleep stages were scored according to the standard Rechtschaffen and Kales criteria (Rechtschaffen and Kales, 1968), and the results were displayed in the usual form as hypnograms.

All signals were recorded either using a TEAC XR-9000 28-channel FM analog tape recorder, a TEAC SR-8000 recorder, or a SONY SIR-1000 32-channel digital recorder. After 350 Hz low-pass filtering, the recordings were subsampled to 150 Hz. For each patient, 480 min of data was available.

For the purposes of this study, spikes were detected by an automatic procedure, applied separately to each channel, which will be briefly described now. The ECoG signal was segmented by a 10 ms sliding window. If the absolute value of the average of the ECoG signal within a segment exceeded a threshold of $100\,\mu V + 5\sigma$ (where σ denotes the standard deviation of the entire dataset for the chosen channel), this segment was labeled as a spike. The performance of this method was evaluated by comparison with the results of visual inspection by an expert. Twenty non-overlapping epochs (epoch length 16.38 s) were consecutively selected from recordings of three sleep stages, and spikes were counted for each individual epoch. If evaluated for all patients, sleep stages and epochs, we obtain for the comparison between automatic and visual spike detection a correlation coefficient of $r = 0.80$, which we consider sufficient for our purpose.

For the purpose of estimating the time-dependent spike rate, individual spikes were counted for non-overlapping epochs of 1 min length; considering the

Table 1
Patient profiles, summary of clinical examinations and outcomes of surgical treatment

Patient #	1	2	3	4	5	6
Age/sex	30/F	29/F	28/M	45/F	25/M	32/M
Seizure type	BS, OA, GTS	BS, OA, GTS	LOC, GTCS	BS, CPS	MA	BS, GCS, CPS
Scalp EEG (including foramen ovale electrode)	Bil. aT spikes (Rt. > Lt.)	Bil. aT spikes	Rt. aT spikes	Bil. aT spikes (Lt. > Rt.)	Bil. aT spikes	Rt. aT spikes
ECoG						
Ictal	Lt. mesial temporal (1 record)	Lt. mesial temporal (4 records)	Lt./Rt. mesial temporal (1/1 record); Lt. basal temporal (6 records)	Lt./Rt. mesial temporal (10/9 records)	Rt. mesial temporal (8 records)	Rt. mesial temporal (1 record)
Inter-ictal	Lt. $\gg$ Rt.	Lt. $\gg$ Rt.	Rt. > Lt.	No clear difference	No clear difference	Rt. > Lt.
MRI	Lt. mesial temporal sclerosis	Lt. mesial temporal sclerosis	No abnormal finding	Lt. mesial temporal sclerosis (mild)	Arachnoid cyst in the Rt. temporal tip; Lt. T3 calcification	No abnormal finding
SPECT	Lt. MTL low	Rt. MTL low	No abnormal finding	Lt. MTL low (slight)	No abnormal finding	Rt. MTL low
Foci	Lt. mesial temporal	Lt. mesial temporal	Rt. temporal	Bilateral mesial temporal	Rt. mesiobasal, Lt. T3	Rt. mesial temporal
Operation	LTL	LTL	RTL	No operation	RTL (additional left T3 cortical tube resection)	RTL
Histopathology	Hippocampal sclerosis	Hippocampal sclerosis	Hippocampal sclerosis	–	Rt. hippocampus gliosis; Lt. temporal lobe ganglioglioma	Hippocampal gliosis
Seizure frequency after operation	Seizure-free	Seizure-free	GTCS one to two times per year CPS-free	–	Seizure-free	Seizure-free

M: male; F: female; BS: blank stare; OA: oral automatism; MA: motion arrest; LOC: loss of consciousness; GTCS: generalized tonic–clonic seizure; GTS: generalized tonic seizure; CPS: complex partial seizure; Bil.: bilateral; Lt.: left; Rt.: right; aT: anterior temporal; (L/R)TL: (left/right) temporal lobectomy; T3: inferior temporal gyrus; MLT: mesian temporal lobe.

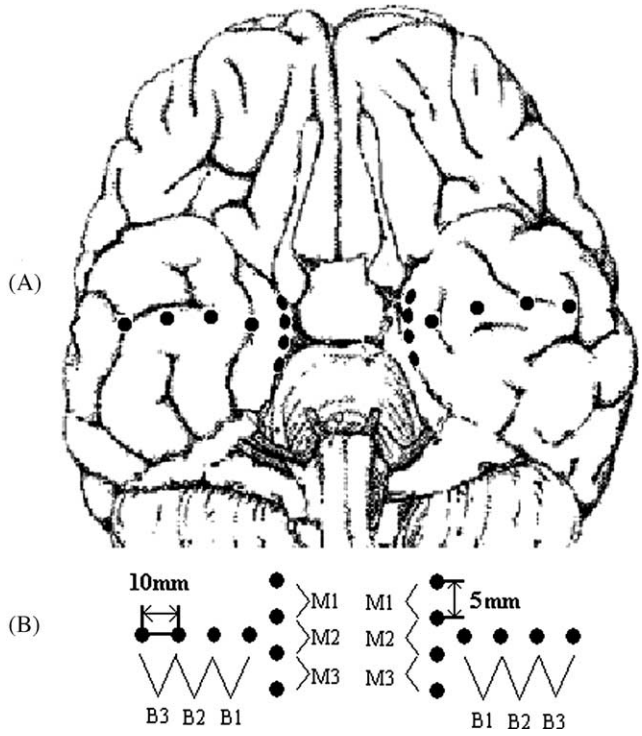

Fig. 1. Electrode positions (A) and ECoG derivations (B). Note that electrode positions approximate, but do not precisely locate each described gyrus. Bipolar recordings of ECoG were used. Six channels are corresponding to each hemisphere.

typical frequency of occurrence of spikes in these recordings, this choice of epoch length represents a reasonable choice.

2.3. Multivariate AR models and attenuation coefficients

In time series analysis, the class of (linear) autoregressive (AR) models is well known for the purpose of linear prediction from a set of p previous values, using a corresponding set of p coefficients.

The generalization of univariate AR models to the case of MAR models is straightforward. The set of previous scalar values is replaced by a set of vectors of simultaneously observed previous values, and the corresponding coefficients are replaced by square matrices. Having estimated these AR coefficient matrices, the impulse response function can be computed. A detailed description of MAR models and of the algorithm for the computation of the impulse response function is given in Appendix A.

MAR models were estimated independently for left and right hemispheres (each containing $N = 6$ channels) based on a segmentation of the given time series into consecutive non-overlapping epochs, and impulse response functions were computed for each epoch. The epoch length was chosen as 3 s (i.e. 450 time frames). In total, for each patient, 9600 epochs within 8 h of nocturnal ECoG were analyzed.

In Fig. 2, some typical epochs and the corresponding impulse response functions are shown. If a given epoch does not contain any spike (Fig. 2(a)), the impulse response function typically will converge to zero (Fig. 2(c)), because all eigenvalues of the corresponding transition matrix (see Eq. (A.6) in Appendix A) will lie inside the unit circle (Fig. 2(e)). On the other hand, if there are spikes in a given epoch (Fig. 2(b)), usually the impulse response function will diverge to infinity (Fig. 2(d)), since some eigenvalues will lie outside the unit circle (Fig. 2(f)). This correspondence between modulus of eigenvalues and behavior of impulse response functions follows

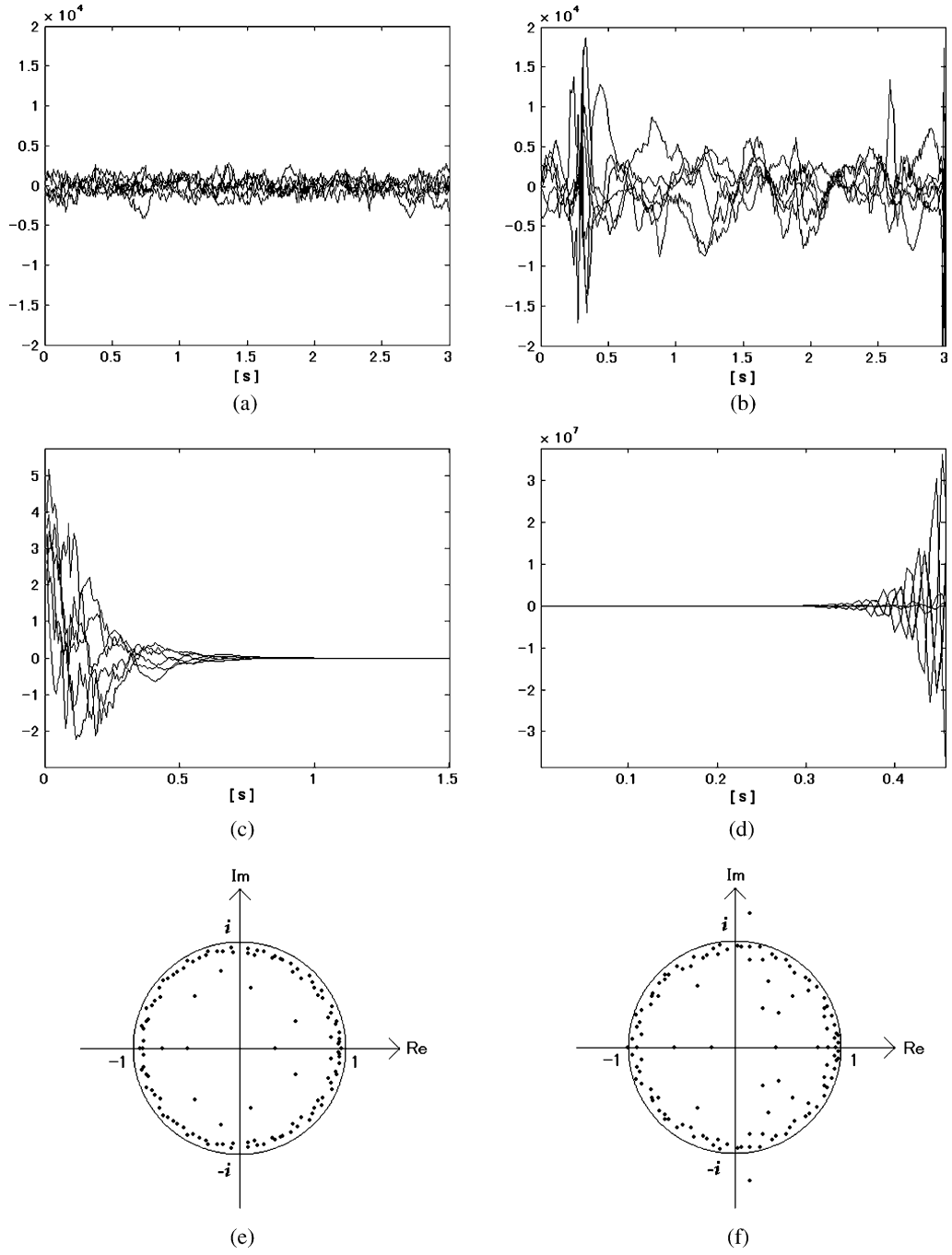

Fig. 2. Superimposed ECoG time series within two epochs without spikes (a) and with spikes (b). Corresponding superimposed impulse response functions (c and d) and corresponding eigenvalues (e and f).

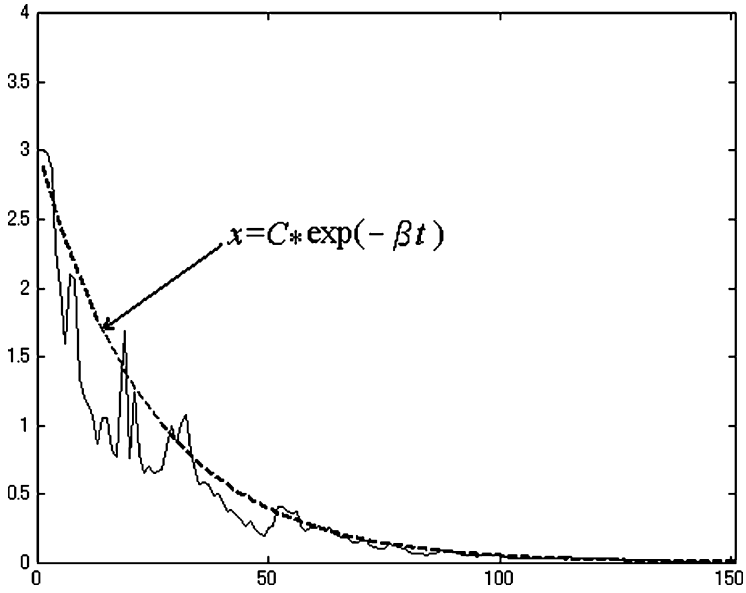

Fig. 3. Averaged absolute value of impulse response functions corresponding to one epoch without spikes (solid line), and fitted damping function (dashed line). Note that by β the attenuation coefficient is denoted.

immediately from linear system theory (Hamilton, 1994).

In order to calculate attenuation coefficients, the absolute values of impulse response functions are averaged over all channels for each epoch; details can be found in Appendix A. Epochs without spikes will typically be characterized by positive values of the attenuation coefficient, see Fig. 3 for an example. The smaller the moduli of the eigenvalues are, the faster will the averaged impulse response function converge to zero, and this will be reflected by a higher value of the attenuation coefficient. However, for epochs containing at least one pronounced spike, the attenuation coefficient is usually found to assume a negative value.

Since it is our interest to study the dynamics of discharge-free background activity in the mesial temporal lobe region, any epoch containing at least one spike was discarded from further analysis. Due to the choice of a very short epoch length of only 3 s, more than 80% of the epochs do not contain any spikes, and the loss of data is negligible. The resulting gaps in the sequence of values of the attenuation coefficient were linearly interpolated by using the values obtained from the two epochs adjacent to the gap; this interpolation step does not affect the results of the analyses to any sizeable extent and serves mainly the purpose of simplifying the numerical implementation.

Before estimating MAR models, the model order p has to be chosen. For the purpose of comparison between models estimated for a large number of different epochs, it would not be advisable to re-adjust the model order for each epoch and each channel, so a common value should be chosen. It is important to choose a sufficiently large value, lest any relevant correlations in the data may be missed. On the other hand, too large model orders may cause over-fitting problems and reduce the reliability of the estimated model parameters due to their large number. We repeated the numerical analyses for values of p ranging from 2 to 40 and found that for $p \geq 20$ results remained essentially unchanged; therefore, we conclude that for our data a model order of $p = 20$ represents a good compromise between the extremes.

We remark that for the given setting the number of parameters which has to be estimated in each individual model fit will exceed the limit of 10% of the number of data points within each epoch; usually, when fitting models to finite data, this case is avoided. But in our case, the models are not fitted for the purpose of prediction, therefore high accuracy of the parameter estimates is not our main concern. The MAR models serve

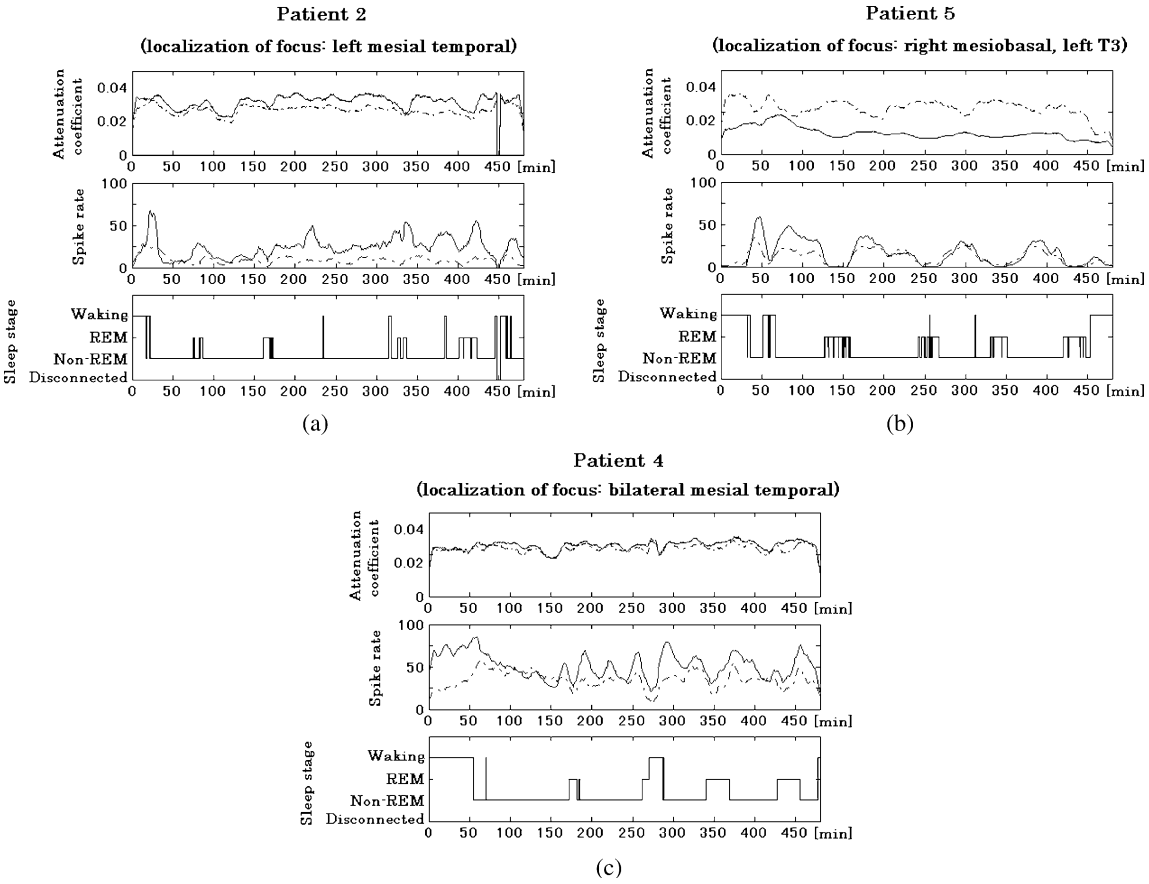

Fig. 4. Temporal evolution of attenuation coefficient (upper panels), spike rate (middle panels) and hypnogram (lower panels) of two typical unilateral focal patients (patient #2 (a) and patient 5# (b)) and the bilateral focal patient (patient #4 (c)). Solid lines and dash-dotted lines are corresponding to left and right hemispheres, respectively. The attenuation coefficient was computed for non-overlapping epochs of 3 s length for nocturnal ECoG data covering 8 h; for the purpose of this graphical representation, the sequence of values of attenuation coefficient was smoothed by a 200-point moving average. Spike rates were counted for non-overlapping epochs of 1 min length and smoothed by a 10-point moving average.

only the purpose of capturing the most salient dynamical properties of the underlying dynamics, which we ultimately summarize in one single number, the attenuation coefficient, therefore we expect the estimates of this coefficient to be sufficiently reliable.

3. Results

Sequences of values of the attenuation coefficient for two typical unilateral patients and one bilateral patient are shown in Fig. 4(a)–(c) (upper panels). In four of the five unilateral focal patients, we find higher values of the attenuation coefficient in the focal hemisphere during almost the entire nocturnal ECoG recordings (including REM, Non-REM and Waking stages, but excluding disconnected periods). However, for the bilateral focal patient the figure shows very similar values of the attenuation coefficient in both hemispheres.

We tested for significance of the difference of attenuation coefficients in epileptic and non-epileptic hemispheres for the set of epochs comprising all REM epochs, all Non-REM epochs and all Waking epochs (denoted by “Complete recording”), without performing any pre-processing, such as applying a moving average (which was done only for the purpose of graphical

Table 2
Evaluation of statistical significance of the difference of AC between focal and non-focal hemispheres (for patient #4 left and right hemispheres) in REM, Non-REM and making epochs, and in all epochs ("Complete recording")

Patient #	Complete recording	REM	Non-REM	Waking
Unilateral				
1	$z = 1.2862$ $P = 0.1745$	$z = 0.9919$ $P = 0.2439$	$z = 0.8045$ $P = 0.2887$	$z = 0.5547$ $P = 0.3421$
2	$z = 3.5762$ $P < 0.0007$[a]	$z = 0.6463$ $P = 0.3237$	$z = 3.4619$ $P = 0.0010$[a]	$z = 0.8659$ $P = 0.2742$
3	$z = 6.4457$ $P < 0.0001$[a]	$z = 4.8248$ $P < 0.0001$[a]	$z = 5.9204$ $P < 0.0001$[a]	$z = 1.3871$ $P = 0.1524$
5	$Z = 11.3356$ $P < 0.0001$[a]	$z = 7.8404$ $P < 0.0001$[a]	$z = 8.9456$ $P < 0.0001$[a]	$z = 3.3565$ $P = 0.0014$[a]
6	$z = 15.7784$ $P < 0.0001$[a]	$z = 4.6296$ $P < 0.0001$[a]	$z = 13.7891$ $P < 0.0001$[a]	$z = 6.7005$ $P < 0.0001$[a]
Bilateral				
4	$z = 1.3796$ $P = 0.1540$	$z = 1.0496$ $P = 0.2300$	$z = 1.1043$ $P = 0.2168$	$z = 0.1490$ $P = 0.3945$

z scores and P-values of standard t-tests are given.
[a] Denotes values with a significance level of more than 95% ($P < 0.05$).

representation). Since for each patient, the total number of epochs was larger than 9000, the standard z-test could be used for this purpose; as null hypothesis, the assumption was used that there was no difference of attenuation coefficient between epileptic and non-epileptic hemispheres. The results are shown in Table 2. From the P-values shown in the table, it can be seen that with respect to "Complete recordings" the discrimination of hemispheres is significant for four of five unilateral patients (#2, #3, #5 and #6). For the case of the only patient failing to show a significant difference (#1), we note that nevertheless the z-value itself is positive, and thereby no contradictory result is produced. Furthermore, even for this patient the attenuation coefficient succeeds to indicate the focal hemisphere correctly in about 50% of all epochs.

For the sake of completeness, Table 2 also contains results obtained only from REM, Non-REM and Waking epochs.

It is possible to obtain additional useful information from analyzing the fluctuations of the attenuation coefficient during time. In Fig. 5, we show the standard deviation (STD) of the sequences of attenuation coefficient values (using all REM and Non-REM epochs) in focal and non-focal hemispheres for all unilateral patients; for the bilateral patient #4, left and right hemispheres are compared. Again for the unilateral patients #2, #3, #5 and #6, standard deviations in the focal hemisphere are higher than in the non-focal hemisphere. In other words, in the focal hemisphere the attenuation coefficient displays larger fluctuations than in the non-focal hemisphere. In the case of bilateral patient #4, the fluctuations of the attenuation coefficient are of approximately the same size in both hemispheres, assuming a similar value as in the focal hemispheres of the unilateral patients.

We shall now discuss some further details of these results. Patient #2 has a focus in the left mesial temporal lobe. As can be seen in Fig. 4(a), middle panel, for this patient the spike rate in the left hemisphere is larger than in right hemisphere. This result agrees well with the results based on the evaluation of the attenuation coefficient.

The recording for patient #5 displays a very regular sleep cycle. As shown in Fig. 4(b), middle panel, there exists a pronounced correlation between the hypnogram and the time course of the spike rate. As mentioned in Section 1, it is well known that Non-REM sleep typically will induce epileptic discharges in the focal hemisphere; in the figure, it can be seen that during REM sleep the spike rate becomes nearly zero. But in contrast to the attenuation coefficient results for this patient, after the first 200 min the spike rate fails to provide clear discrimination between focal and non-focal

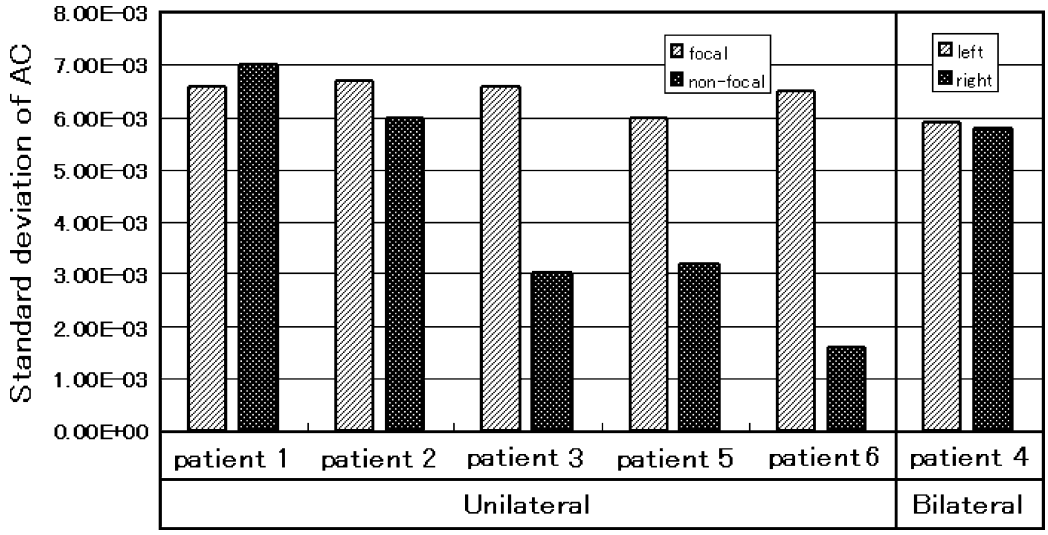

Fig. 5. Standard deviation of sequences of attenuation coefficient (AC) corresponding to focal and non-focal hemispheres (left and right bars, respectively), for patient #4 corresponding to left and right hemispheres.

hemispheres; moreover, in contradiction to the medical diagnosis, during the first 200 min of this recording, the spike rate in the non-focal hemisphere turns out to be higher than in the focal hemisphere (note that in Fig. 4(b), middle panel, within the first 200 min the solid line attains larger values than the dash-dotted line). Therefore, we surmise that the attenuation coefficient may provide an improved criterion for detecting the focal hemisphere correctly; from Table 2, it can be seen that for this patient significant results are obtained even if only REM, Non-REM or Waking epochs are considered. Furthermore, we also find in the focal hemisphere a noticeable correlation between the attenuation coefficient and the hypnogram: during REM sleep, the values of the attenuation coefficient are higher than during Non-REM sleep. Therefore, the difference between the attenuation coefficients of focal and non-focal hemispheres is larger during REM sleep compared to Non-REM sleep.

From Table 2, it can be seen that for patient #4 the difference of attenuation coefficients between left and right hemispheres does not show statistical significance; as shown in Fig. 4(c), upper panel, in contrast to the unilateral patients, for patient #4, values of attenuation coefficient are fluctuating synchronously in both hemispheres. However, the spike rate in the left hemisphere is frequently higher than in the right hemisphere, see Fig. 4(c), middle panel; this fact is also mentioned in Table 1 for the case of scalp EEG from the same patient. In summary, we find that for these patients the attenuation coefficient provides a more coherent and conclusive characterization of brain state than the spike rate.

4. Discussion

The main topic of the present study is the investigation of the linear dynamical properties of basic background ECoG activity in patients suffering from mesial temporal lobe epilepsy. Based on the results of this investigation, we have proposed a new method for detecting the focal hemisphere. More specifically, we found that in four out of five unilateral patients the dynamics of spike-free background activity displays significantly higher attenuation coefficient in the focal hemisphere than in the non-focal hemisphere. Furthermore, in a patient showing a regular sleep cycle these differences were higher during REM sleep than during Non-REM sleep.

The results presented in this study indicate that basic background activity without any obvious epileptic wave patterns may contain relevant information for the detection of the focal hemisphere in temporal lobe epilepsy. Since in this study we have employed a database composed of a limited number of

patients, further studies employing larger databases will be needed in order to investigate whether this approach may be useful in clinical practice. It would also be desirable to apply this approach to ECoG recordings obtained from larger numbers of implanted electrodes.

Since our study focuses on the analysis of nocturnal recordings, it also bears relevance for certain aspects concerning the relationship between sleep stage and epileptic phenomena. The spike rate is affected by various physiological conditions. It is known that Non-REM sleep induces epileptic discharges. However, for certain patients having an irregular sleep cycle, sometimes this phenomenon is not observed. Based on the results of our preliminary study, we conjecture that analysis of the background activity by the attenuation coefficient may facilitate the distinction between the hemispheres in such cases, presumably because the dynamics underlying the background ECoG activity reflects the temporary brain state of the patient.

Since the level of cortical activity during wakefulness is comparable to that during REM sleep, also attenuation coefficient analysis of awake-state data may provide useful information. Especially for patients #5 and #6, significant *z*-values were found during Waking epochs, and we note that for all unilateral patients *z*-values during Waking epoch are higher than for the bilateral patient. In the present study, we only have analyzed sleep ECoG data with some interspersed short instances of waking, therefore a detailed investigation of awake-state data should be the subject of future research.

It would also be interesting to investigate whether similar information could be obtained also from scalp EEG. In this study, we have used cortical signals recorded from electrodes attached directly to the parahippocampal gyrus. This area is very close to the hippocampus, which is considered as an area likely to contain the focus or foci of mesial temporal epilepsy. On the other hand, for the case of scalp EEG the electrode closest to the epileptic focus is given by the anterior temporal derivation, but this position is still much farther away from the focus than the locations of the intracranial electrodes, as used in this study. Another problem is that the amplitude of the scalp EEG is at least five times smaller than the amplitude of the ECoG, and furthermore the EEG is contaminated by diffuse electric fields and various artifacts originating from eye movements, blinking, muscle activity, electrocardial signals and other sources. For these reasons, when applied to EEG data the performance of the attenuation coefficient may be less favorable than in the case of ECoG data. Nevertheless, in future work our approach should be extended to scalp EEG data.

Finally, we would like to add some comments on the results presented in this study from the viewpoint of system theory. Those aspects of brain dynamics which can be captured by the sets of intracranial electrodes employed in this study, have been represented for each hemisphere by a MAR model, and the properties of these models have been summarized by their averaged impulse response functions; if an external force, such as an impulse, was applied to these MAR models, the ensuing oscillation would decay faster for the focal hemisphere than for the non-focal hemisphere. In other words, a high value of the attenuation coefficient is correlated to higher robustness and stability against disturbances.

Currently, the limited size of the database used in our study, both with respect to number of patients and number of electrodes, still renders these results preliminary; but if we may provisionally presume their validity, a tentative physiological interpretation of these differences of dynamical properties could be provided by assuming a decrease of dynamical flexibility in the focal hemisphere, possibly caused by histological degeneration and deficiencies of neuronal networks (Sloviter, 1994; Bahh et al., 1999), furthermore by hilar cell loss and mossy fiber reorganization (Masukawa, 1999). As a result of this increased dynamical stiffness of such neuronal networks, their dynamics would be less affected by impulses and therefore could recover more quickly than in the case of unimpaired networks. Wang and Wieser (1994) found reduced fluctuation of the background EEG (recorded by foramen ovale electrodes) in the focal hemisphere, as compared to the non-focal hemisphere. Essentially, the conclusions of their study are in agreement with our results.

However, we have also demonstrated by our study of nocturnal ECoG that within the focal hemisphere, in spite of its rigidity, pronounced changes depending on sleep stage do occur.

As an alternative to our approach, it would be possible to carry out in vivo experiments in animal or human tissue, in order to directly observe the impulse response elicited by adding electrical stimuli during basic background activity of the neural tissue. However, it is to be

expected that such electrical stimuli would interact with the background activity and possibly change the dynamical properties of the neural tissue. For this reason, the approach of conducting additional experiments for the purpose of obtaining improved observations leads to a difficult situation, known as the "observation problem" in physics. Thus, mathematical modeling of actual data and analyzing the corresponding dynamical properties through numerical simulation is to be preferred, since it will avoid this problem. Accordingly, we find that the approach of analyzing time series by MAR models provides useful information about the dynamics of the system, which cannot be obtained from experiments.

Acknowledgements

The authors would like to express their sincere thankfulness to Dr. Rolando J. Biscay Lirio (Institute of Cybernetics, Mathematics and Physics, Havana, Cuba) for helpful discussions and comments on the manuscript, and to the anonymous referees for valuable comments and suggestions that have led to a considerable improvement of this paper. Support from the Japan Society for the Promotion of Science (JSPS) through fellowship grants 00065 (2001) and P 03059, and from the German Research Council (DFG) through grant GA 673/1-1 is acknowledged.

Appendix A

Suppose that x_t denotes a time series of observed scalar values, where t denotes time. A univariate autoregressive (AR) model for x_t is defined by

$$x_t = \sum_{i=1}^{p} a_i x_{t-i} + e_t, \tag{A.1}$$

where p denotes model order, a_i denotes the AR coefficients and e_t represents prediction error. The AR coefficients are estimated by a standard least-squares method, such that the sum of squares of e_t is minimized.

The generalization of univariate AR models to the case of MAR models is straightforward. Suppose that $\boldsymbol{X}_t = (x_t^1, x_t^2, \ldots, x_t^N)^{\mathrm{T}}$ denotes the vector of simultaneously measured values at time t (where N denotes the number of channels), then the corresponding MAR model is given by the vector equation

$$\boldsymbol{X}_t = \sum_{i=1}^{p} \boldsymbol{A}_i \boldsymbol{X}_{t-i} + \boldsymbol{E}_t. \tag{A.2}$$

Here, the AR coefficients $\boldsymbol{A}_i$ are no longer scalar quantities as in the case of univariate AR models, but have become matrices. $\boldsymbol{E}_t$ is a prediction error vector for all channels: $\boldsymbol{E}_t = (e_t^1, e_t^2, \ldots, e_t^N)^{\mathrm{T}}$. Through the MAR model of Eq. (A.2), each channel of the time series $\boldsymbol{X}_t$ is described by

$$x_t^l = \sum_{i=1}^{p} \sum_{m=1}^{N} a_i^{lm} x_{t-i}^m + e_t^l, \quad l = 1, \ldots, N. \tag{A.3}$$

The AR coefficients can be estimated by a similar method as in the case of univariate AR models.

The state space notation of the MAR model Eq. (A.2) is given by

$$\begin{aligned}
&\boldsymbol{Z}_t = \boldsymbol{\Phi} \boldsymbol{Z}_{t-1} + \boldsymbol{V}_t, \quad \text{where} \\
&\boldsymbol{Z}_t = (\boldsymbol{X}_t^{\mathrm{T}}, \boldsymbol{X}_{t-1}^{\mathrm{T}}, \ldots, \boldsymbol{X}_{t-p+1}^{\mathrm{T}})^{\mathrm{T}}, \\
&\boldsymbol{Z}_{t-1} = (\boldsymbol{X}_{t-1}^{\mathrm{T}}, \boldsymbol{X}_{t-2}^{\mathrm{T}}, \ldots, \boldsymbol{X}_{t-p}^{\mathrm{T}})^{\mathrm{T}}, \\
&\boldsymbol{V}_t = \left(\boldsymbol{E}_t \overbrace{(0, \ldots, 0)}^{N \times p} \right)^{\mathrm{T}},
\end{aligned} \tag{A.4}$$

and $\boldsymbol{\Phi}$ denotes the state transition matrix which is defined as

$$\boldsymbol{\Phi} = \begin{pmatrix} \boldsymbol{A}_1 & \boldsymbol{A}_2 & \ldots & \boldsymbol{A}_p \\ \boldsymbol{I} & \boldsymbol{0} & \ldots & \boldsymbol{0} \\ \vdots & \ldots & \ddots & \vdots \\ \boldsymbol{0} & \ldots & \boldsymbol{I} & \boldsymbol{0} \end{pmatrix}. \tag{A.5}$$

Here, $\boldsymbol{X}$ and $\boldsymbol{A}$ are the same as in Eq. (A.2).

Eq. (A.5) implies that

$$\boldsymbol{Z}_{t+s} = \boldsymbol{\Phi}^s \boldsymbol{Z}_{t-1} + \sum_{i=0}^{s-1} \boldsymbol{\Phi}^i \boldsymbol{V}_{t+s-i}. \tag{A.6}$$

The first N rows of the vector equation represented by Eq. (A.6) constitute a vector generalization of Eq. (A.2)

$$\boldsymbol{X}_{t+s} = \sum_{i=1}^{p} \boldsymbol{\Phi}_{1i}^{(s)} \boldsymbol{X}_{t-i+1} + \sum_{j=0}^{s-1} \boldsymbol{\Psi}_j \boldsymbol{E}_{t+s-j}. \tag{A.7}$$

Here, $\boldsymbol{\Psi}_j = \boldsymbol{\Phi}_{11}^{(j)}$, and $\boldsymbol{\Phi}_{11}^{(j)}$ denotes the upper left block of $\boldsymbol{\Phi}^j$, where $\boldsymbol{\Phi}^j$ is the matrix $\boldsymbol{\Phi}$ raised to the jth power; that is to say that the matrix $\boldsymbol{\Phi}_{11}^{(j)}$ is composed of rows 1 through N and columns 1 through N from the matrix $\boldsymbol{\Phi}^j$. More generally, $\boldsymbol{\Phi}_{1i}^{(j)}$ is composed of rows 1 through N and columns $(i-1)N+1$ through iN from the matrix $\boldsymbol{\Phi}^j$.

The impulse response function of the vector Eq. (A.4) is defined as

$$\boldsymbol{Z}_s = \boldsymbol{\Phi}^s \boldsymbol{Z}_0, \quad \text{where}$$

$$\boldsymbol{Z}_0 = \left(\overbrace{(1, \ldots, 1)}^{N} \overbrace{(0, \ldots, 0)}^{N\times(p-1)} \right)^{\mathrm{T}}. \tag{A.8}$$

If the eigenvalues of $\boldsymbol{\Phi}$ all lie inside the unit circle, then $\boldsymbol{\Phi}^s \to 0$ as $S \to \infty$, therefore $\boldsymbol{Z}_s \to 0$ (Hamilton, 1994).

In order to calculate attenuation coefficients, the impulse response functions are averaged over all channels for each epoch (after taking absolute values), resulting in a new function $x(t)$ (where t denotes time), to which then a damping function is directly fitted by a standard least-squares method

$$x(t) = C \exp(-\beta t) \tag{A.9}$$

Here, C denotes an irrelevant amplitude parameter, and β denotes the attenuation coefficient.

References

Akaike, H., 1981. Recent development of statistical methods for spectrum estimation. In: Yamaguchi, N., Fujisawa, K. (Eds.), Recent Advances in EEG and EMG Data Processing. Elsevier/North-Holland Biomedical Press, pp. 63–78.

Akiyama, Y., Mori, K., Baba, H., Ono, K., 1995. Prediction of postoperative EEG changes for intractable epilepsy through a multidimensional autoregressive analysis. No Shinkei Geka 23, 587–593.

Bahh, B.E., Lespinet, V., Lutron, D., Coussemacq, M., Salle, G.L., Rougier, A., 1999. Correlations between granule cell dispersion, mossy fiber sprouting, and hippocampal cell loss in temporal lobe epilepsy. Epilepsia 40, 1393–1401.

Chokroveerty, S., 1994. Sleep and epilepsy. In: Chokroveerty, S. (Ed.), Sleep Disorders Medicine. Butterworths–Heinemann, Boston, pp. 429–454.

Franaszczuk, P.J., Bergey, G.K., 1998. Application of the directed transfer function method to mesial and lateral onset temporal lobe seizures. Brain Topogr. 11, 13–21.

Galka, A., 2000. Topics in Nonlinear Time Series Analysis — With Implications for EEG Analysis. World Scientific, Singapore.

Gath, I., Feuerstein, C., Pham, D.T., Rondouin, G., 1992. On the tracking of rapid dynamic changes in seizure EEG. IEEE Trans. Biomed. Eng. 39, 952–958.

Gersch, W., Yonemoto, J., Naitoh, P., 1977. Automatic classification of multivariate EEGs using an amount of information measure and the eigenvalues of parametric time series model features. Comput. Biomed. Res. 10, 297–318.

Grassberger, P., Procaccia, I., 1983. Characterization of strange attractors. Phys. Rev. Lett. 50, 346–349.

Hamilton, J.D., 1994. Time Series Analysis. Princeton University Press, Princeton.

Hernandez, J., Valdes-Sosa, P.A., Vila, P., 1996. EEG spike and wave modeled by a stochastic limit cycle. NeuroReport 7, 2246–2250.

Isaksson, A., Wennberg, A., Zetterberg, L.H., 1981. Computer analysis of EEG signals with parametric models. Proc. IEEE 69, 451–461.

Kaminski, M.J., Blinowska, K.J., 1991. A new method of the description of the information flow in the brain structures. Biol. Cybern. 65, 203–210.

Lehnertz, K., Elger, C.E., 1995. Spatio-temporal dynamics of the primary epileptogenic area in temporal lobe epilepsy characterized by neuronal complexity loss. Electroencephalogr. Clin. Neurophysiol. 95, 108–117.

Liberati, D., Cursi, M., Locatelli, T., Comi, G., Cerutti, S., 1997. Total and partial coherence analysis of spontaneous and evoked EEG by means of multi-variable autoregressive processing. Med. Biol. Eng. Comput. 35, 124–130.

Lopes da Silva, F., 1987. EEG analysis: theory and practice. In: Niedermeyer, E., Lopes da Silva, F. (Eds.), Electroencephalography. Urban and Schwartzenberg, Baltimore/Munich, pp. 613–618.

Masukawa, L.M., 1999. Physiological and anatomical correlates of the human dendate gyrus: consequences of causes of epilepsy. In: Delgado-Escueta, A.V., Wilson, W.A. (Eds.), Jasper's Basic Mechanisms of the Epilepsies: Advances in Neurology, third ed., vol. 79. Lippincott, Williams & Wilkins, Philadelphia, pp. 781–794.

Medvedev, A., Willoughby, J.O., 1999. Autoregressive modeling of the EEG in systemic kainic acid-induced epileptogenesis. Int. J. Neurosci. 97, 149–167.

Miwakeichi, F., 2001. Characterization of spike & wave signals in epileptic EEG: a non-linear non-parametric time series approach. Ph.D. thesis, Department of Statistical Science, School of Mathematical and Physical Science, The Graduate University for Advanced Studies.

Miwakeichi, F., R-Padron, R., Valdes-Sosa, P.A., Ozaki, T., 2001. A comparison of non-parametric models for epilepsy data. Comput. Biol. Med. 31, 41–57.

Montplaisir, J., Laveerdiere, M., Saint-Hilaire, J., Rouleau, I., 1987. Nocturnal sleep recording in focal epilepsy: a study with depth electrodes. J. Clin. Neurophysiol. 4, 383–388.

Niedermeyer, E., 1987. Depth electroencephalography. In: Niedermeyer, E., Lopes da Silva, F. (Eds.), Electroencephalography. Urban and Schwartzenberg, Baltimore/Munich, pp. 593–612.

Rechtschaffen, A., Kales, A., 1968. A manual of standardised terminology, techniques and scoring system for sleep stages of human subject. In: Rechtschaffen, A., Kales, A. (Eds.), Brain Information Service. Brain Research Institute, Los Angeles.

Repucci, M.A., Schiff, N.D., Victor, J.D., 2001. General strategy for hierarchical decomposition of multivariate time series: implications for temporal lobe seizures. Ann. Biomed. Eng. 29, 1135–1149.

Shimizu, H., Suzuki, I., Ohta, I., Ishijima, B., 1992. Mesial temporal subdural electrode as a substitute for depth electrode. Surg. Neurol. 38, 186–191.

Sloviter, R.S., 1994. The functional organization of the hippocampal dentate gyrus and its relevance to the pathogenesis of temporal lobe epilepsy. Ann. Neurol. 35, 640–654.

Speckmann, E.J., Elger, C.E., 1987. Introduction to the neurophysiological basis of the EEG and DC potentials. Urban and Schwartzenberg, Baltimore/Munich.

Velasco, M., Brito, F., Jimenez, F., Gallegos, M., Velasco, A.L., Velasco, F., 1995. Sleep–epilepsy interactions in patients with intractable generalized tonic seizures and depth electrodes in the centromedial thalamic nucleus. Arch. Med. Res. 26, 117–125.

Wang, J., Wieser, H.G., 1994. Regional “rigidity” of background EEG activity in the epileptogenic zone. Epilepsia 35, 495–504.

Weber, B., Lehnertz, K., Elger, C.E., Wieser, H.G., 1998. Neuronal complexity loss in interictal EEG recorded with foramen ovale electrodes predicts side of primary epileptogenic area in temporal lobe epilepsy: a replication study. Epilepsia 39, 922–927.

Wieser, H., 1991. Temporal lobe epilepsy, sleep and arousal: stereo-EEG findings. In: Degen, R., Rodin, E.A. (Eds.), Epilepsy, Sleep and Sleep Deprivation. Elsevier, Amsterdam, pp. 97–119.